Original Paper

Brain, Behavior and Evolution

Brain Behav Evol
DOI: 10.1159/000365960

Received: April 29, 2014
Returned for revision: May 25, 2014
Accepted after second revision: July 16, 2014
Published online: November 12, 2014

Retinal Ganglion Cell Distribution and Spatial Resolving Power in Deep-Sea Lanternfishes (Myctophidae)

Fanny de Busserolles[a, c] N. Justin Marshall[b] Shaun P. Collin[a]

[a]School of Animal Biology and the Oceans Institute, The University of Western Australia, Crawley, W.A., and
[b]Sensory Neurobiology Group, Queensland Brain Institute, The University of Queensland, St. Lucia, Qld., Australia;
[c]Red Sea Research Centre, King Abdullah University of Science and Technology, Thuwal, Saudi Arabia

Key Words
Retinal ganglion cell · Amacrine cell · Spatial resolving power · Myctophid · Retinal topography · Stereology · Deep sea · Evolutionary history · Teleost

Abstract
Topographic analyses of retinal ganglion cell density are very useful in providing information about the visual ecology of a species by identifying areas of acute vision within the visual field (i.e. areas of high cell density). In this study, we investigated the neural cell distribution in the ganglion cell layer of a range of lanternfish species belonging to 10 genera. Analyses were performed on wholemounted retinas using stereology. Topographic maps were constructed of the distribution of all neurons and both ganglion and amacrine cell populations in 5 different species from Nissl-stained retinas using cytological criteria. Amacrine cell distribution was also examined immunohistochemically in 2 of the 5 species using anti-parvalbumin antibody. The distributions of both the total neuron and the amacrine cell populations were aligned in all of the species examined, showing a general increase in cell density toward the retinal periphery. However, when the ganglion cell population was topographically isolated from the amacrine cell population, which comprised up to 80% of the total neurons within the ganglion cell layer, a different distribution was revealed. Topographic maps of the true ganglion cell distribution in 18 species of lanternfishes revealed well-defined specializations in different regions of the retina. Different species possessed distinct areas of high ganglion cell density with respect to both peak density and the location and/or shape of the specialized acute zone (i.e. elongated areae ventro-temporales, areae temporales and large areae centrales). The spatial resolving power was calculated to be relatively low (varying from 1.6 to 4.4 cycles per degree), indicating that myctophids may constitute one of the less visually acute groups of deep-sea teleosts. The diversity in retinal specializations and spatial resolving power within the family is assessed in terms of possible ecological functions and evolutionary history.

Introduction

Retinal topographic analyses of the distribution of neurons within the ganglion cell layer are very useful in providing information on how animals perceive and process visual information. Using the wholemount technique [Stone, 1981; Coimbra et al., 2006; Ullmann et al.,

KARGER

E-Mail karger@karger.com
www.karger.com/bbe

0006–8977/14/0000–0000$39.50/0

Fanny de Busserolles
4700 King Abdullah University of Science and Technology
Ibn Al Haytham Bldg., Room 3216 WS-15
Thuwal 23955-6900 (Saudi Arabia)
E-Mail fanny.debusserolles@kaust.edu.sa

2011], which allows examination of the entire retina, areas of high cell density or retinal specialization can be identified. These areas of high cell density provide greater acuity in a specific part of the visual field and usually closely reflect each species' habitat and behavioural ecology in both terrestrial and aquatic vertebrates [Hughes, 1977; Collin and Pettigrew, 1988a, b, 1989; Bozzano and Collin, 2000; Collin and Shand, 2003]. The spatial distribution of ganglion cells can form specializations such as an 'area' or a 'streak'. An area is a region of acute vision formed by a concentric increase in cell density in a specific part of the retina usually found in species living in a three-dimensional, 'enclosed' environment [Hughes, 1977; Collin and Pettigrew, 1988a] and exhibiting predatory behaviour [Fritsches et al., 2003]. Conversely, horizontal streaks, which are formed by an elongated increase in cell density across the retinal meridian, allow an animal to scan a broad horizon (panoramic field) with enhanced acuity without using distinctive eye movements [Hughes, 1977; Collin and Pettigrew, 1988b]. This type of specialization is usually found in species living in an open environment, where they perceive their surroundings with an uninterrupted view of the horizon, defined in the ocean by the air-water or sand-water interfaces [Collin and Shand, 2003].

The deep sea, and more particularly the mesopelagic zone, is a relatively simple visual environment, reliant on essentially two different light sources: the residual downwelling sunlight and bioluminescence. Downwelling sunlight between 200 and 1,000 m diminishes exponentially with depth, creating a semi-extended visual scene where shadows (prey, predators or conspecifics) can be detected against the lighter background when viewed from below. Bioluminescent emissions, on the other hand, which are produced by a large range of organisms, occur at all depths and are thought to play important roles in the deep sea, subserving behavioural interactions with prey, predators and congeners [Herring, 2002; Haddock et al., 2010].

Although the deep-sea environment does not support as high a biodiversity as the well lit, shallow water environment, many deep-sea species possess a wide range of retinal specializations to allow acute vision in specific parts of the visual field [Collin and Partridge, 1996; Collin et al., 1997; Wagner et al., 1998]. Areae have been found in several tubular and non-tubular eyed deep-sea species of teleosts, providing acute vision in different parts of the visual field depending on the location of the specialization [Collin and Partridge, 1996; Wagner et al., 1998]. A fovea, a pit-like invagination of the retina associated with an area, has also been observed in several species [Collin and Partridge, 1996; Wagner et al., 1998; Collin et al., 2000], providing high acuity and possibly image magnification, accurate fixation and depth perception [Walls, 1942]. Finally, relatively unspecialiszed retinas with a nearly uniform ganglion cell distribution, probably mediating high sensitivity rather than acuity, have also been reported in a single group of deep-sea fishes, the Myctophidae [Wagner et al., 1998].

Myctophids or lanternfishes are one of the most abundant groups of mesopelagic fishes occupying all of the world's oceans. Like most mesopelagic organisms, they are bioluminescent and possess two kinds of bioluminescent structures (i.e. photophores and luminous organs) thought to play several different roles (camouflage, distraction, illumination and intra- and inter-specific communication) [Case et al., 1977; Edwards and Herring, 1977]. Myctophids also show marked intra- and interspecific variation in the depths they occupy [Karnella, 1987], their migration patterns [Watanabe et al., 1999] and the location of their luminous organs [Nafpaktitis and Nafpaktitis, 1969; Paxton, 1972; Nafpaktitis et al., 1977, 1978; Zahuranec, 2000; Herring, 2007; de Busserolles et al., 2013]. Recently, marked differences in the visual system of this large group of fishes have been revealed [de Busserolles et al., 2013, 2014a, b], including large variations in photoreceptor distribution across the retina [de Busserolles et al., 2014b].

The first study examining the distribution of neurons within the ganglion cell layer in lanternfishes revealed a concentric increase in cells toward the periphery, potentially enhancing acute vision around the peripheral visual field [Collin and Partridge, 1996]. Although this type of cell arrangement might appear as a good strategy in an environment where small bioluminescent flashes can appear from any direction and at any time, it was later revealed that this specialization did not represent the true distribution of ganglion cells due to the inclusion of an unusually large population of displaced amacrine cells. Once the amacrine cell population was removed, analysis of the distribution of true ganglion cells revealed a rather unspecialized retina with a weak area centralis [Collin and Hoskins, 1997; Wagner et al., 1998]. However, these analyses were only realized for 3 different species of lanternfishes, all belonging to the same genus, *Lampanyctus,* which might only represent one type of retinal specialization within this large family. In this study, we investigate the diversity of the visual system of lanternfishes by examining the distribution and density of the true ganglion cell population in a large range of lanternfish species from

different genera. We also examine the contribution of the 'displaced' amacrine cell population to the total number of neurons present in the ganglion cell layer. The diversity in retinal specializations and spatial resolving power (SRP) within the family is discussed in terms of possible ecological functions and evolutionary history.

Materials and Methods

Collection of Species and Preservation of Ocular Tissue

Samples were obtained from several research cruises in the Coral Sea (RV Cape Ferguson) under the following collection permits: Coral Sea waters (CSCZ-SR-20091001-01), Commonwealth waters (AU-COM2009051), GBRMPA (G09/32237.1) and Queensland Fisheries (133805) (Marshall, AEC #SNG/080/09/ARC) and the Peru-Chile trench (FS Sonne, sampling permits were obtained by the Chief Scientist, University of Tübingen). For all specimens, sampling was carried out following the guidelines of the NHMRC Australian Code of Practice under an animal ethics protocol of The University of Western Australia (RA/3/100/917). Additional specimens from Western Australian waters, the Tasman Sea and the Bay of Biscay were acquired through collaborators.

For each individual, the standard length, rostro-caudal eye diameter (measured in situ) and lens diameter were measured with digital calipers to 0.1 mm. For most of the lanternfishes, measurements were performed on fresh specimens on board ship prior to dissection and fixation. However, when samples were acquired from collaborators, the measurements and dissection were made after fixation. Depending on the source of the samples, tissue was fixed in 4% paraformaldehyde in 0.1 M phosphate buffer (PB; pH 7.4), 5% buffered formalin or Karnovsky's fixative (2.5% paraformaldehyde and 2% glutaraldehyde in 0.1 M cacodylate buffer, pH 7.4). Since formaldehyde has previously been found to affect body length by only 0.8% [Kristoffersen and Salvanes, 1998], no measurement corrections were used between fresh and fixed specimens.

Preparation of Retinal Wholemounts and Nissl Staining

Retinal wholemounts were prepared according to standard protocols [Stone, 1981; Coimbra et al., 2006; Ullmann et al., 2011]. Radial cuts were performed in order to flatten the eye and subsequently the retina in toto onto a glass slide, where the orientation was confirmed by making a small additional cut in the nasal or dorso-nasal part of the eye. The sclera, retinal pigment epithelium and tapetum (when present) were gently removed with the help of No. 3 watchmaker's forceps and a Kolinsky hair paintbrush. The retina was wholemounted on a gelatinized slide, with the ganglion cell layer facing up. In order to improve cell differentiation, wholemounts were left to dry at room temperature overnight in formalin vapours and incubated for an additional hour in formalin vapour at 60°C prior to staining [Stone, 1981; Coimbra et al., 2006, 2012]. Following the staining protocol of Coimbra et al. [2006], wholemounts were rehydrated, stained in 0.1% cresyl violet for 5 min, dehydrated in an ethanol series, cleared in xylene, and mounted with Entellan New (Merck). Since retinal wholemounts were attached to the slide during all of the staining steps, shrinkage was considered negligible and (where present) confined to the retinal margins [Coimbra et al., 2006].

Amacrine Cell Labelling Using Immunohistochemistry

Parvalbumin antibody was used to selectively label amacrine cells present in the ganglion cell layer of 2 species of lanternfishes, i.e. *Ceratoscopelus warmingii* and *Myctophum asperum*. Retinal wholemounts, fixed in 4% paraformaldehyde, were dissected as described above and rinsed 3 times in 0.1 M PB (5 min each). In order to optimize the immunolabelling, 2 pre-treatments were performed: antigen retrieval and endogenous peroxidase inactivation. Briefly, each wholemount was first incubated in boric buffer at 60°C for 30 min, cooled to room temperature for 5 min and incubated for 15 min in a light tight vial containing a solution of 10% methanol and 3% H_2O_2 in 0.1 M PB [Coimbra et al., 2012]. Retinas were then permeabilized in 5% Triton-X-100 solution (2 × 5 min followed by 1 × 20 min) [Coimbra et al., 2012] before being rinsed 3 times (for 5 min each) in 0.1 M PB. Retinal wholemounts were incubated under gentle rocking at room temperature for 24 h in a solution containing anti-parvalbumin (1:1,000, product No. P3088, mouse monoclonal; Sigma-Aldrich, USA), 0.3% Triton and 5% rabbit serum (Vector Laboratories, USA), in 0.1 M PB. Thereafter, the retinas were washed 3 times in 0.1 M PB (5 min each) and further incubated for 1 h in a mixture of biotinylated rabbit anti-mouse secondary antibody (1:200; Jackson ImmunoResearch, USA) with 0.3% Triton in 0.1 M PB. Finally, retinal wholemounts were incubated in an avidin/biotin complex (Vectastain ABC Kit; Vector Laboratories) for 1 h and rinsed 3 times in 0.1 M PB (5 min each) before being reacted with nickel-enhanced 3,3 diaminobenzidine solution (DAB Kit; Vector Laboratories). Each retina was then wholemounted on a gelatinized slide, dried overnight, dehydrated in an ethanol series, cleared in xylene, and mounted with Entellan New (Merck).

Anti-parvalbumin immunolabelling was also performed on retinal sections of *C. warmingii* in order to verify the specificity of the labelling. Briefly, a piece of retina was cryoprotected by sequential incubations (5 min each) in a graded series of sucrose solution (10, 20 and 30% in 0.1 M PB). After a 24-hour incubation at 4°C in 30% sucrose, the sample was embedded in OCT Tissue-Tek medium (Sakura Finetek, USA) and 20-μm sections were cut using a Leica CM1900 cryostat-microtome and mounted on a microscope slide. Immunolabelling was performed directly on the slides as described above for the wholemount with the exception of the pretreatments, which are unnecessary on sections. Following the reaction, the sections were mounted in 40% glycerol in 0.1 M PB and observed using light microscopy.

Photographs of the Nissl-stained and immunolabelled retinal wholemounts and sections of *C. warmingii* were taken using a digital video camera (MicroFIRE; OPTRONICS) mounted on a compound microscope (Olympus BX50). For display purposes only, the contrast and brightness of the entire photographs were adjusted using Adobe Photoshop CS4 (Adobe System Inc., USA).

Stereological Analyses and the Construction of Topographic Maps

The total number and topographic distribution of the total neuron, amacrine cell and ganglion cell populations present within the ganglion cell layer of several species of lanternfishes were assessed using the optical fractionator technique [West et al., 1991] modified by Coimbra et al. [2009, 2012] for use in wholemounted

Table 1. Summary of the parameters used for the analysis of neural cell distribution

Species	Individuals	SL, mm	Eye ∅, mm	Counting frame size, μm	Grid size, μm	Site No.	CE for GC	CE for AC	CE for TC
C. warmingii	1	44.1	4.1	50×50	320×320	190	0.040	0.030	0.031
	2	38.6	3.5	50×50	280×280	185	0.029	0.026	0.025
	3	36.3	3.5	50×50	270×270	186	0.032	0.031	0.029
	3*					202		0.036	
M. asperum	1	78.4	8.5	50×50	750×750	165	0.037	0.033	0.030
	1*					183		0.041	
B. nikolayi	1	37.7	4.1	50×50	340×340	201	0.033	0.031	0.029
D. laternatus	1	19.3	1.9	50×50	140×140	180	0.034	0.033	0.032
N. kroeyerii	1	95.2	6.1	75×75	550×550	202	0.024	0.026	0.023

TC = Total neural cells; AC = amacrine cells; GC = ganglion cells, SL = standard length; ∅ = diameter. * Retina analysed with parvalbumin immunohistochemistry to label amacrine cells.

retinas. Briefly, the retinal wholemount was considered as a single section (section sampling fraction = 1), and since the neurons are organized in a single layer (ganglion cell layer), the thickness sampling fraction was fixed at 1. The outline of the retinal wholemount was then digitized using a ×4 objective (numerical aperture 0.13) mounted on a compound microscope (Olympus BX50) equipped with a motorized stage (MAC5000; Ludl Electronics Products, USA), a digital video camera (MicroFIRE; OPTRONICS), and a computer running Stereo Investigator software (Microbrightfield, USA). Using a ×60 oil immersion objective (numerical aperture 1.35), cells were randomly and systematically counted using the parameters listed in tables 1 and 2. The total number of cells was estimated by multiplying the sum of total neurons counted by the area of the sampling fraction (i.e. ratio between the counting frame and the sampling grid) [West et al., 1991; Coimbra et al., 2009].

Three types of cells can be identified and distinguished within the ganglion cell layer based on cytological criteria from Nissl-stained retinas: ganglion cells, amacrine cells and glial cells [Hughes, 1975; Collin, 1988; Collin and Pettigrew, 1988c]. Ganglion cells are characterized by their larger size, irregular shape and large nucleus with a granular appearance. Amacrine cells are characterized by their small size, round or teardrop shape and darkly stained appearance, whereas glial cells are differentiated by their distinctive elongated shape. While glial cells are easily discriminated from the other cells, amacrine cells can sometimes be hard to distinguish confidently from ganglion cells based on cytological criteria alone, and as a result they are often included in topographic analyses. Fortunately, several studies have shown that the distribution of amacrine cells in the ganglion cell layer matches the distribution of the true ganglion cells and that consequently their inclusion in the neural cell counts does not change the overall topography [Wong and Hughes, 1987; Collin and Pettigrew, 1988c; Bailes et al., 2006b; Coimbra et al., 2006; Collin, 2008]. However, lanternfishes seem to be an exception to this rule. In fact, lanternfishes seem to possess a very large proportion of amacrine cells in the ganglion cell layer (up to 80%) [Collin and Hoskins, 1997; Wagner et al., 1998; Bozzano et al., 2007], which masks the distribution of the true ganglion cell population [Collin and Hoskins, 1997; Wagner et al., 1998].

In this study, we confirmed the distribution of the amacrine cell population in another 5 species of lanternfishes and estimated their proportion. To do so, we used the Stereo Investigator system to simultaneously count amacrine cells and ganglion cells at each sampling site in 5 species (table 1). Amacrine cells and ganglion cells were differentiated using the cytological criteria described previously (fig. 1) and using two different markers. Using this approach, we were able to generate data for amacrine cells alone, ganglion cells alone and both amacrine and ganglion cells together (total neural cells). For 2 of the 5 species, i.e. *C. warmingii* and *M. asperum,* immunolabelled amacrine cells present in the ganglion cell layer were counted from the complementary retina (right eye), using the same stereological criteria (table 1), to validate the distribution obtained using Nissl staining (left eye). Due to the consistent discrepancy found between amacrine and ganglion cell distributions, we chose to only count ganglion cells in the remaining 12 species analysed. Subsampling was carried out in the area of highest cell density to estimate the peak density of ganglion cells. Intraspecific variability in ganglion cell distribution was investigated for 3 species, i.e. *C. warmingii, Electrona risso* and *Myctophum obtusirostre,* for which 2–3 different individuals were analysed.

The counting frame and grid size were chosen carefully in order to maintain the highest level of sampling and achieve an acceptable Schaeffer coefficient of error (CE). The CE is a measure of the accuracy of the total number of cell estimates and is considered acceptable below 0.1 [Glaser and Wilson, 1998; Slomianka and West, 2005]. As a result, the grid size was modified between each species to allow sampling of around 200 sites per retina and to enable us to compare different-sized individuals in the case of *C. warmingii* and *E. risso.* The counting frame size was also adjusted between species to allow a minimum average count of 40 cells per sampling site. However, due to the large proportion of amacrine cells, the counting frame used to count amacrine cells and ganglion cells simultaneously in the 5 species investigated (50 × 50 or 75 × 75 μm; table 1) did not always allow this for ganglion cells. To avoid this

Table 2. Summary of the parameters used for the analysis of the ganglion cell distribution along with Schaeffer's CE

Species	Individuals	SL, mm	Eye ∅, mm	Counting frame size, μm	Grid size, μm	Site No.	Schaeffer's CE
C. warmingii	1	44.1	4.1	100×100	320×320	198	0.033
	2	38.6	3.5	100×100	280×280	199	0.030
	3	36.3	3.5	100×100	270×270	196	0.029
E. risso	1	n.a.	n.a.	100×100	680×680	205	0.039
	2	n.a.	n.a.	100×100	850×850	202	0.041
B. longipes	1	42.1	4.0	100×100	350×350	207	0.026
B. nikolayi	1	37.7	4.1	100×100	340×340	201	0.033
D. mollis	1	66.2	6.5	100×100	580×580	200	0.029
D. parri	1	35.2	4.1	100×100	330×330	204	0.033
D. laternatus	1	19.3	1.9	50×50	140×140	180	0.034
L. luminosa	1	104.3	8.4	150×150	800×800	181	0.023
L. alatus	1	49.8	3.3	75×75	295×295	197	0.045
L. parvicauda	1	54.2	3.3	75×75	260×260	211	0.040
M. asperum	1	78.4	8.5	100×100	750×750	172	0.034
M. brachygnathum	1	67.7	7.7	100×100	600×600	206	0.045
M. lychnobium	1	51	5.0	100×100	400×400	165	0.043
M. nitidulum	1	77.9	6.9	100×100	650×650	168	0.042
M. obtusirostre	1	92.3	10.6	100×100	850×850	197	0.046
	2	90.88	10.5	100×100	850×850	173	0.050
M. spinosum	1	60.7	5.1	100×100	500×500	159	0.041
N. kroeyerii	1	95.2	6.1	100×100	550×550	206	0.024
S. rufinus	1	73.7	6.3	100×100	500×500	198	0.035

SL = Standard length; ∅ = diameter; n.a. = not available.

problem and assess ganglion cell distribution confidently in these 5 species, ganglion cells were counted a second time, separately (with the exception of *Diogenichthys laternatus*), using a larger counting frame (100 × 100 μm; table 2).

Topographic maps were constructed using the statistical program R v.2.15.0 (R Foundation for Statistical Computing, 2012) with the results exported from the Stereo Investigator software according to Garza Gisholt et al. [2014]. Garza Gisholt et al. [2014] proposed 4 methods of spatial analysis giving representations similar to construct isodensity maps. For this study, we chose to use the Gaussian Kernel Smoother from the Spatstat package [Baddeley and Turner, 2005]. For each map, the sigma value was adjusted to the distance between points (i.e. grid size).

Phylogenetic Comparison of Visual Characteristics

In order to assess the influence of phylogeny on inter-specific variability in retinal specializations within the Myctophidae, we mapped the type of specialization (or area of high ganglion cell density) onto an existing phylogeny [Paxton et al., 1984] including all of the species examined here and in a previous study [Wagner et al., 1998]. Paxton et al. [1984] published a phylogeny classifying genera using derived character states of adult osteology and photophore patterns [Paxton, 1972] and of larvae [Moser and Ahlstrom, 1970, 1972, 1974] and it is currently the most up-to-date morphological phylogeny.

Calculation of the SRP

The upper limit of SRP was estimated for each species using the peak density of ganglion cells, as described by Pettigrew and Collin [1989]. Briefly, since Matthiessen's ratio states that the focal length f in teleosts fishes is about 2.55 the radius of the lens [Matthiessen, 1882, 1886], the angle subtending 1 mm on the retina (angle α) can be calculated using the following formula:

$$\alpha = \arctan(1/f).$$

Knowing the peak density of ganglion cells (PGC in cells/mm^2), angle α and the fact that at least 2 ganglion cells are needed to distinguish the boundary of a black and white cycle of a grating, we can calculate the SRP in cycles per degree:

$$SRP = (PGC/\alpha)/2.$$

Results

Immunolabelling of Amacrine Cells in the Lanternfish Retina

Immunolabelling using anti-parvalbumin revealed the presence of 2 populations of amacrine cells, a low-density population in the inner nuclear layer and a high-density population in the ganglion cell layer (fig. 2). The morpho-

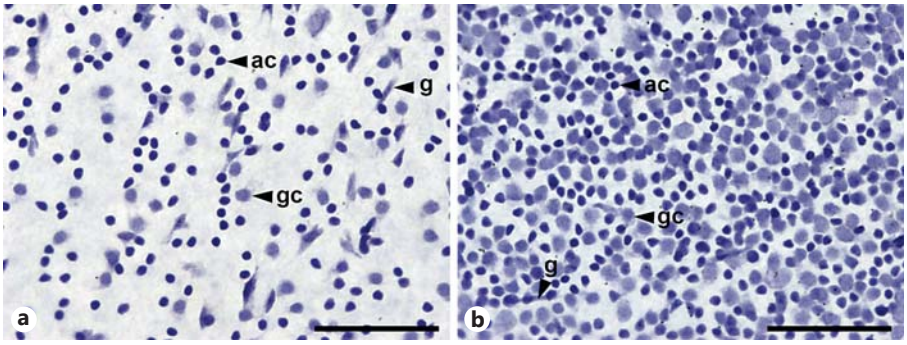

Fig. 1. Light micrographs of the Nissl-stained ganglion cell layer of *C. warmingii* in a low-density area (nasal part; **a**) and in the peak-density area (temporal; **b**). gc = Ganglion cell; ac = amacrine cell; g = glial cell. Scale bars = 50 μm.

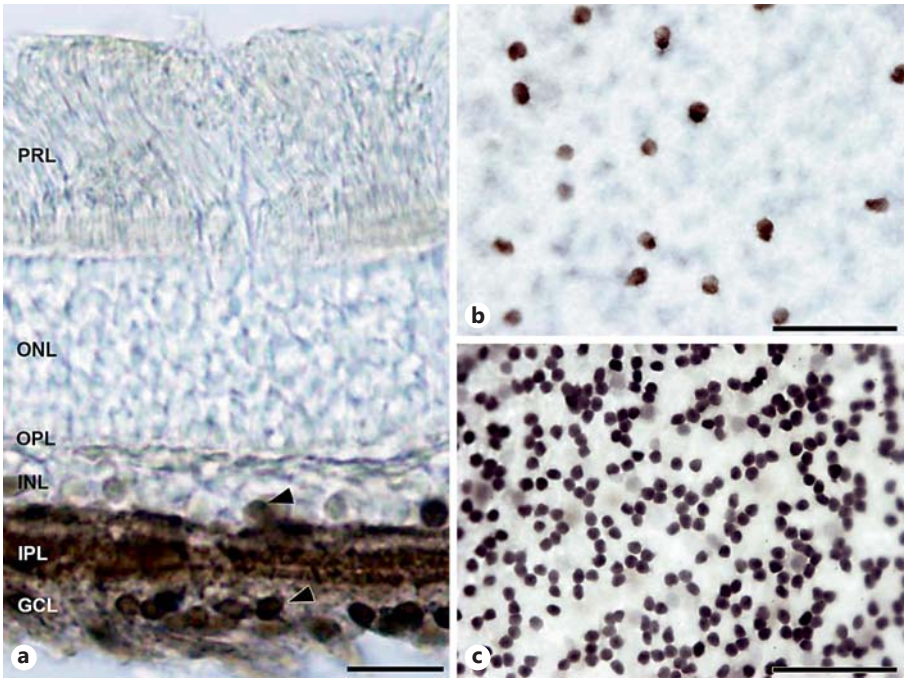

Fig. 2. Light micrographs from a transverse section (**a**) and a wholemount (**b**, **c**) of the amacrine cells, immunolabeled with anti-parvalbumin, in the retina of *C. warmingii*. **a** The arrowheads indicate the location of the amacrine cells in the inner nuclear layer (INL) and the ganglion cell layer (GCL). **b** Amacrine cells labelled in the INL. **c** Amacrine cells labelled in the GCL. PRL = photoreceptor layer; ONL = outer nuclear layer; OPL = outer plexiform layer; IPL = inner plexiform layer. Scale bars = 20 μm (**a**) and 50 μm (**b**, **c**).

logical aspect of the cells labelled with parvalbumin antibody was very similar to the amacrine cells identified in the ganglion cell layer of the Nissl-stained retinas using cytological criteria (small round or teardrop-shaped cells; fig. 1, 2). Within the ganglion cell layer, the staining intensity of the immunolabelled amacrine cells varied from light staining to dark staining possibly indicating the presence of different types of amacrine cells (fig. 2c).

Analyses of the amacrine cell distribution within the ganglion cell layer using both immunolabelling and Nissl staining revealed very similar results in terms of topography, with both species showing a concentric increase in amacrine cells toward the periphery (online suppl. fig. 1; see www.karger.com/doi/10.1159/000365960 for all online suppl. material). However, small discrepancies in the total number of amacrine cells were observed between both methods (~7% difference; table 3).

Neural Cell Distribution in the Ganglion Cell Layer of Lanternfishes

Topographic maps of total neural cells, amacrine cells and ganglion cells, present in the ganglion cell layer of 5 different species of lanternfishes, were constructed from Nissl-stained retinal wholemounts where amacrine cells and ganglion cells were counted simultaneously. Since the results were similar between the 5 species (listed in table 3) in terms of total neural cell and amacrine cell distributions, only results for *M. asperum* are presented here (fig. 3). Results for the 4 remaining species are provided in the supplementary material (online suppl. fig. 2), and their ganglion cell topography is presented later.

Topographic maps of *M. asperum* showed that both total neural cell and amacrine cell topographies were aligned where the concentric increase in cells toward the periphery were in register (fig. 3a, b). However, when

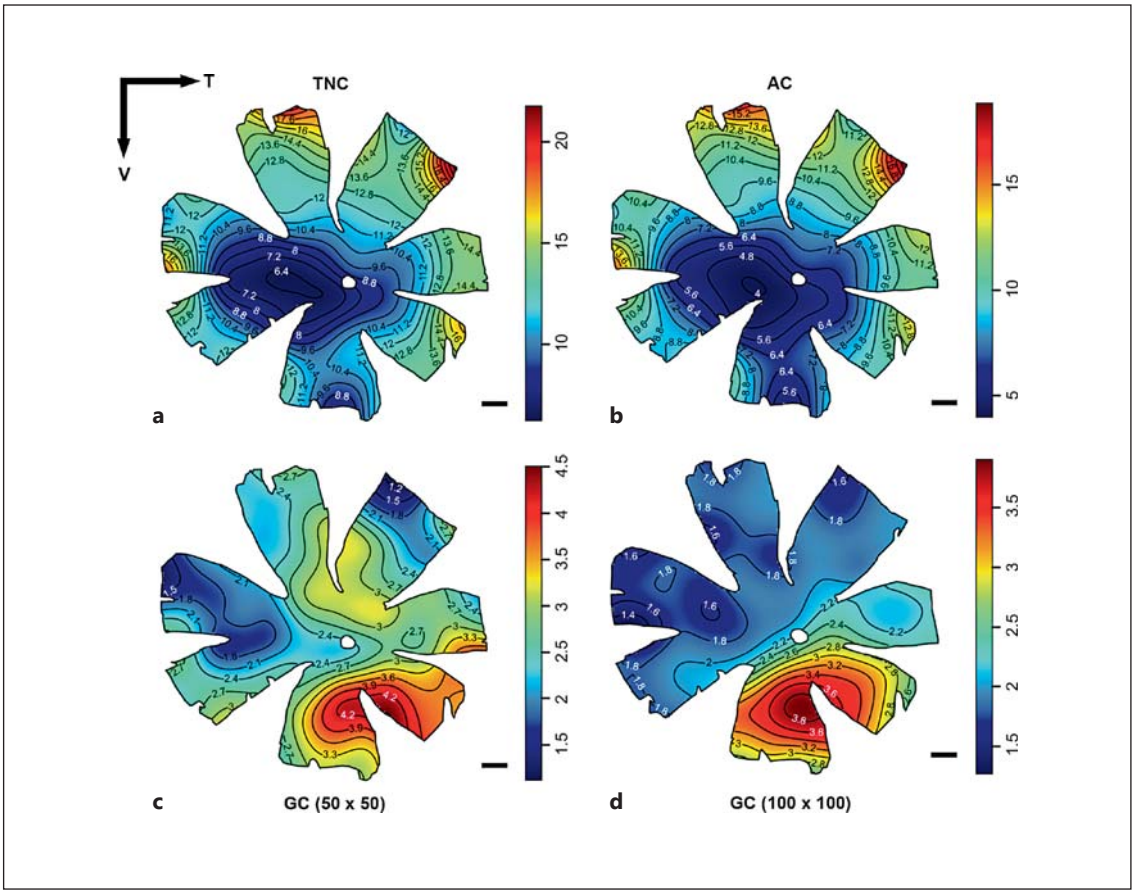

Fig. 3. Topographic distribution of the total neural cells (**a**), amacrine cells (**b**) and ganglion cells (**c**, **d**) of *M. asperum*. The maps were produced using the same Nissl-stained wholemount and grid (750 × 750 μm). Two different counting frames were used: 50 × 50 μm (**a–c**) and 100 × 100 μm (**d**). The black lines represent isodensity contours, and values are expressed in densities × 10^3 cells/mm^2. The arrows indicate the orientation of the retina. T = Temporal; V = ventral; TNC = total neural cells; AC = amacrine cells; GC = ganglion cells. Scale bars = 1 mm.

Table 3. Summary of the neural cell (ganglion, amacrine and total neural cell populations) quantitative data obtained using the optical fractionator method on the wholemounted retinas of 5 species of lanternfishes

Species	Individuals	Total GC, n	Total AC, n	Total cells, n	AC, %
C. warmingii	1	83,927	296,755	380,682	78
	2	90,755	279,762	370,518	76
	3	79,198	221,266	300,464	74
	3*		254,829		
M. asperum	1	248,625	809,325	1,057,950	77
	1*		706,500		
B. nikolayi	1	123,738	276,515	400,253	69
D. laternatus	1	28,937	58,925	87,863	67
N. kroeyerii	1	152,352	544,446	696,799	78

GC = Ganglion cells; AC = amacrine cells. * Retina analysed with parvalbumin immunohistochemistry to label amacrine cells.

Table 4. Summary of the ganglion cell quantitative data obtained using the optical fractionator method on the wholemounted retinas of 18 species of lanternfishes

Species	Individuals	Peak cell density, cells/mm^2	Mean cell density, cells/mm^2	Total cells, n	Lens ∅, mm	SRP
C. warmingii	1	11,000	3,662	74,255	1.6	2.0
	2	14,300	5,215	81,355	1.4	2.0
	3	13,200	5,247	74,970	1.4	2.0
E. risso	1	8,000	2,402	227,685	3.4	3.4
	2	5,200	1,695	247,311	4.4	3.6
B. longipes	1	14,900	5,244	132,973	1.8	2.6
B. nikolayi	1	20,100	5,156	123,738	1.8	3.0
D. mollis	1	7,200	1,945	130,859	3.2	3.1
D. parri	1	17,400	4,697	104,347	1.8	2.8
D. laternatus	1	23,200	8,204	28,937	0.7	1.6
L. luminosa	1	4,577	1,990	230,599	3.7	2.8
L. alatus	1	19,600	8,227	141,065	1.3	2.3
L. parvicauda	1	23,600	8,918	127,051	1.4	2.6
M. asperum	1	5,200	1,958	189,394	3.7	3.0
M. brachygnathum	1	10,600	3,256	241,452	3.3	3.9
M. lychnobium	1	8,200	3,916	103,392	2.3	2.4
M. nitidulum	1	8,500	2,023	143,608	3.1	2.9
M. obtusirostre	1	6,900	1,998	284,448	4.7	4.4
	2	9,000	2,706	338,202	4.5	4.8
M. spinosum	1	9,100	3,969	157,750	2.5	2.7
N. kroeyerii	1	6,000	2,304	141,721	2.7	2.4
S. rufinus	1	11,200	4,269	211,325	2.8	3.4

∅ = Diameter.

only the ganglion cells were mapped, a totally different pattern was revealed, with most cells distributed in the ventral area (fig. 3c). *M. asperum* also provides a good example of how important the choice of counting frame is when the gradient of cells is relatively shallow (1,200–4,500 ganglion cells/mm^2). As mentioned in Materials and Methods, the counting frame chosen to simultaneously count amacrine cells and ganglion cells together (i.e. 50 × 50 μm; table 1) only allowed us to count a very small proportion of ganglion cells per sampling site (less than 20 cells on average per site). As a result, even though the Schaeffer coefficient is acceptable (<0.05), ganglion cell counts in the regions of low cell density revealed a specialization in the dorsal part of the retina (fig. 3c) that does not exist (fig. 3d) if a larger counting frame (i.e. 100 × 100 μm; table 2) is used, allowing a larger number of ganglion cells to be counted in each sampling site (an average of at least 40 cells per site).

In terms of cell number, the total number of neural cells (ganglion cells plus amacrine cells) varied greatly between species and ranges from 87,863 cells *(D. laternatus)* to 1,057,950 cells *(M. asperum)* and is positively correlated with eye size (tables 1, 3). Similar levels of variation and a correlation with eye size were observed for the total number of ganglion cells and amacrine cells when assessed separately. However, the amacrine cell population was very large compared to the ganglion cell population, representing between 67 and 78% of the total neural cells present within the ganglion cell layer (table 3).

Intra- and Inter-Specific Differences in Ganglion Cell Distribution

Intra-specific variability in ganglion cell topography was assessed in 3 species, i.e. *C. warmingii* (3 individuals), *E. risso* (2 individuals) and *M. obtusirostre* (2 individuals). Although differences in cell numbers and densities were observed between individuals of the same species (tables 1–4), the general ganglion cell topography varied little (online suppl. fig. 3), allowing comparison between individuals. However, since slight orientation errors can be made when preparing wholemounts (adhering them to the slide in the exact dorso-ventral orientation in which they sit in the eye/head) and because only one individual per species was analysed in most cases, we only attempted

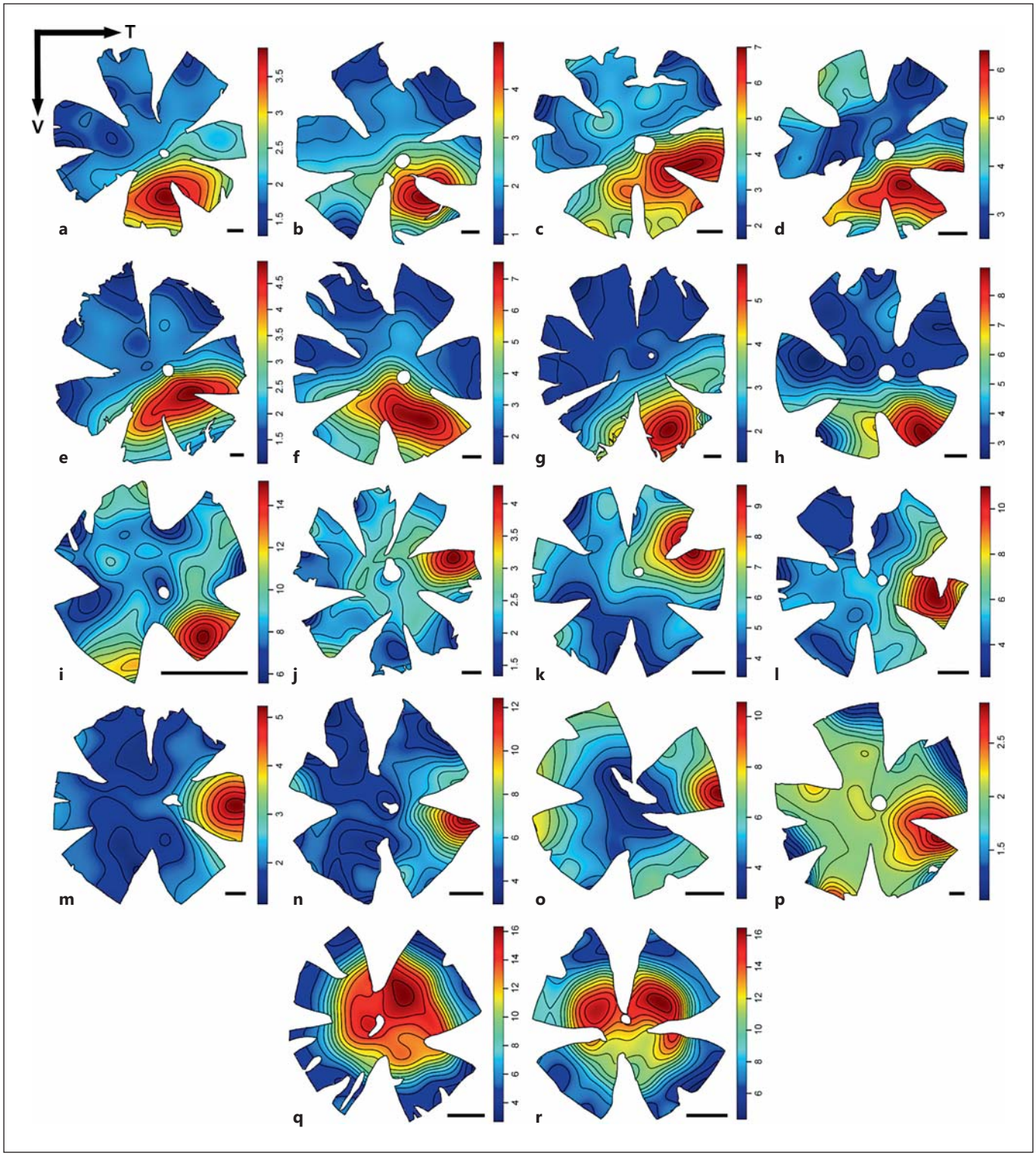

Fig. 4. Topographic distribution of retinal ganglion cells in 18 species of lanternfishes. **a** *M. asperum*. **b** *M. nitidulum*. **c** *M. spinosum*. **d** *M. lychnobium*. **e** *M. obtusirostre*. **f** *M. brachygnathum*. **g** *E. risso*. **h** *S. rufinus*. **i** *D. laternatus*. **j** *Notoscopelus kroeyerii*. **k** *B. longipes*. **l** *B. nikolayi*. **m** *D. mollis*. **n** *D. parri*. **o** *C. warmingii*. **p** *L. luminosa*. **q** *L. alatus*. **r** *L. parvicauda*. The black lines represent isodensity contours, and values are expressed in densities × 10^3 cells/mm^2. The arrows indicate the orientation of the retina. T = Temporal; V = ventral. Scale bars = 1 mm.

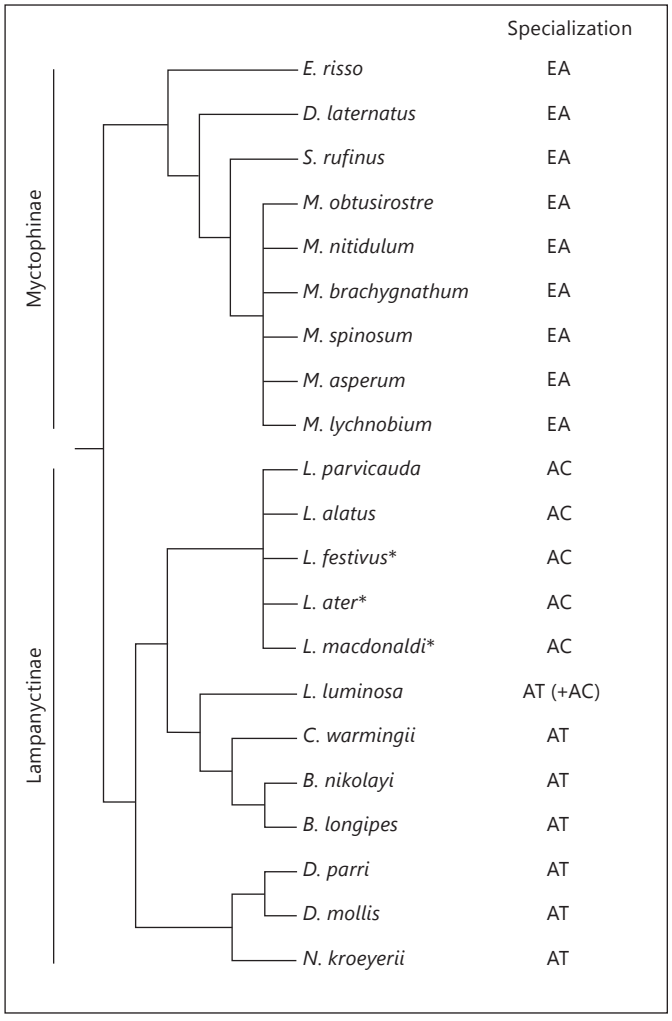

Fig. 5. Type of retinal specialization in each of the 18 species of lanternfishes analysed and plotted against the phylogeny of Paxton et al. [1984]. EA = Elongated area; AC = area centralis, AT = area temporalis. * Data from Wagner et al. [1998].

to compare the general ganglion cell pattern (main specialization) between species. Topographic analysis of the ganglion cell distribution of 18 different species of lanternfishes revealed 3 main specializations defined by their shape and location within the retina: (1) elongated areae temporo-ventrales or an area of high cell density that decreases in an elongated fashion in the temporo-ventral region of the retina, (2) areae temporales or a high cell density arranged in a concentric fashion in the temporal part of the retina and (3) large areae centrales or large areas of high cell density arranged in a concentric fashion in the centre of the retina (fig. 4). Based on these criteria, an elongated area was found in the ventro-temporal part of the retina in 9 species (*M. asperum, M. nitidulum, M. spinosum, M. lychnobium, M. obtusirostre, M. brachygnathum, E. risso, Symbolophorus rufinus* and *D. laternatus;* fig. 4a–i). An area temporalis was observed in 7 species, i.e. *Bolinichthys longipes, B. nikolayi, Diaphus mollis, D. parri, Lampadena luminosa, N. kroeyerii* and *C. warmingii* (fig. 4j–p). Finally, a large area centralis with a gradual decrease in cells toward the periphery was observed in the remaining 2 species, i.e. *Lampanyctus alatus* and *L. parvicauda,* with a peak density located centrally and extending towards the dorso-temporal part of the retina (fig. 4q, r).

We consider it important to assess the influence of phylogeny on the type of retinal specialization, especially given the paucity of information regarding the behaviour and life history traits of each species. Therefore, we mapped the 3 main specialization types and locations onto an existing phylogenetic tree [Paxton et al., 1984] that includes all of the species examined to date [Wagner et al., 1998; this study] (fig. 5). The type of retinal specialization appears to follow closely the phylogeny, with species from the Myctophinae subfamily possessing only elongated areae ventro-temporales, and representatives of the subfamily Lampanyctinae having both areae centrales and areae temporales. Even within the subfamily Lampanyctinae, the type of specialization is well partitioned along the phylogeny, with areae centrales found exclusively within the genus *Lampanyctus* and areae temporales found in the remaining genera. This is further supported by the presence of an intermediate species showing the transition from an area centralis to an area temporalis, i.e. *L. luminosa* which possesses an area temporalis and a decrease in cells toward the periphery similar to the area centralis observed in *Lampanyctus* species.

The total number of ganglion cells varies greatly between species, ranging from 28,937 cells *(D. laternatus)* to 284,448 cells (*M. obtusirostre*; table 4), and it seems to vary directly with eye size (tables 2, 4). Mean and peak cell densities also vary greatly between species (from 1,958 to 8,918 cells/mm^2 and from 5,200 to 23,600 cells/mm^2, respectively; table 4). However, contrary to the total cell number, they do not appear to vary according to eye size.

Spatial Resolving Power

The SRP was estimated using the peak ganglion cell density for each species (table 4). The SRP was relatively low in myctophids, varying from 1.63 cycles per degree *(D. laternatus)* to 4.38 cycles per degree *(M. obtusirostre)*. Interestingly, the species possessing the highest ganglion cell density *(L. parvicauda)* did not have the highest SRP. SRP was positively correlated with eye size and lens diam-

eter. The intra-specific variability in the estimated SRP was very low, with a standard deviation of 0.04 *(C. warmingii).*

Discussion

Ecological Significance of the Retinal Specializations in Lanternfishes

Analysis of retinal ganglion cell distribution, including the determination of regions of high cell densities (i.e. specializations), is a powerful means of investigating how a species visually samples its environment [Hughes, 1977; Collin and Pettigrew, 1988a, b; Collin, 2008]. The distribution of the true ganglion cell population (not including amacrine cells) has previously been examined in 3 species of lanternfish from the genus *Lampanyctus* [Collin and Hoskins, 1997; Wagner et al., 1998]. Although the topographic maps of ganglion cells were not provided in these studies, the authors reported a poorly specialized retina, showing a nearly uniform distribution of cells within the ganglion cell layer, with the presence of an area centralis in all 3 species. In concordance with these studies, we found an area centralis in another 2 *Lampanyctus* species. However, although the gradient of cells was relatively shallow in all species, we showed that the myctophid retina is indeed specialized, highlighting the presence of 2 additional specializations (an elongated area ventro-temporalis and an area temporalis).

The retinal morphology of teleost fishes is highly diverse and usually correlated with habitat complexity and behavioural ecology [Collin and Pettigrew, 1988a, b; Collin, 1997]. In the mesopelagic zone, habitat complexity is relatively low and mainly influenced by the intensity gradient of the residual downwelling sunlight along the vertical axis. Differences in retinal specializations are therefore more likely due to inter-specific differences in behaviour. Unfortunately, very limited information is available on the behavioural ecology of members of this family. However, hypotheses on the function of the retinal specializations found in myctophids can be made.

While a horizontal streak will allow an animal to scan a broad horizon with enhanced acuity without using distinctive eye movements [Hughes, 1977; Collin and Pettigrew, 1988a, b], areae provide acute vision in a specific part of the visual field. Several lanternfish species possess an elongated area, i.e. an intermediate specialization between a streak and an area. Assuming a horizontal position of the fish in the water column, a ventro-temporal elongated area will subtend the frontal and dorsal view of the visual field, allowing the detection of silhouettes situated above them against the lighter background of the upper mesopelagic zone.

Color version available online

Fig. 6. Frontal view of the head of *D. mollis* showing the presence of large ventro-nasal (Vn) luminous organs (the two large white tissue patches in front of the eyes). The position of the eyes, slightly tilted forward, most likely allows binocular vision in the frontal visual field.

Areae temporales improve the acuity of the visual field situated in front of the fish and may facilitate binocular vision in species living in a structurally complex habitat or exhibiting predatory behaviours [Hughes, 1977; Collin and Pettigrew, 1988a, b; Fritsches et al., 2003]. Myctophids are predatory species, feeding on a wide range of organisms (mainly zooplankton but also fishes) [Podrazhanskaya, 1993]. However, it is unknown how myctophids catch their prey. It has been suggested that species possessing head luminous organs (i.e. *Diaphus* sp.) may use their organs as head torches in order to search for prey [Herring, 1985]. *D. mollis,* for example, possesses large ventro-nasal (Vn) luminous organs most likely emitting light directly in front of the fish (fig. 6). The area temporalis found in *D. mollis* (this study), associated with the presence of a nasal aphakic gap [de Busserolles et al., 2014a], provides the potential for binocular vision (fig. 6) and may enhance acuity directly in the illuminated region in front of the fish, a powerful predatory strategy.

A large area centralis was found in 2 species of lanternfishes, i.e. *L. alatus* and *L. parvicauda,* indicating a higher

acuity in the centro-lateral visual field thereby allowing the fish to perceive signals in a large part of its monocular field of view, suggesting that these species are visual generalists. In addition to the generalist specialization, *L. parvicauda* does not appear to possess a very sensitive visual system due to its relatively small eyes [de Busserolles et al., 2013] and low summation ratios (around 20:1 in the peak area and 50:1 in the periphery) compared to other myctophids (i.e. *M. brachygnathum* 200:1 in the peak area and 500:1 in the non-specialized region) [de Busserolles et al., 2014b; this study]. Even though *L. parvicauda* possesses adaptations to enhance photon capture over the whole retina (i.e. circumlental aphakic gap and tapetum lucidum) [de Busserolles et al., 2014a], these findings indicate that this species possesses a less specialized visual system than the 2 other species mentioned above. Wagner [2001] investigated brain areas in mesopelagic fishes and showed that different myctophid species rely more or less heavily on different sensory systems. *L. ater,* for example, which possesses a visual specialization similar to the 2 *Lampanyctus* species analysed in this study [Wagner et al., 1998], seems to mainly rely on its gustatory sense [Wagner, 2001], while *D. mollis* relies principally on exteroception and vision. Consequently, *L. parvicauda* and, to some extent, the other *Lampanyctus* species might not rely as much on vision and might instead depend more heavily on other sensory systems to survive in the mesopelagic zone.

SRP in Lanternfishes

The SRP in lanternfishes is relatively low (1.3–4.8 cycles per degree) [Wagner et al., 1998; this study] compared to other deep-sea teleosts, i.e. tubular and non-tubular eyes, which range from 4.3 to 22.9 cycles per degree [Collin and Partridge, 1996; Collin et al., 1997; Wagner et al., 1998]. However, the estimation of SRP for these other deep-sea teleosts did include the amacrine cell population, which could have resulted in an overestimation. Nevertheless, even if the peak total neural cell population (ganglion cells plus amacrine cells) is taken into consideration when estimating SRP in lanternfishes (i.e. 20,000 instead of 5,000 cells/mm^2 in *M. asperum*), the myctophid SRP would still be low compared to other deep-sea species. Moreover, the proportion of amacrine cells estimated in 2 tubular-eyed species was reported to be relatively low (less than 20%) [Locket, 1977; Collin et al., 1998], reinforcing the fact that lanternfishes might constitute one of the less acute groups of deep-sea fishes. Similar to shallow-water and deep-sea tubular-eyed species [Collin and Pettigrew, 1989; Collin et al., 1997], the SRP in myctophids was also found to vary in proportion to eye/lens size.

Collin and Pettigrew [1989] found a relationship between SRP and feeding strategies in 12 different species of reef teleosts, with species not requiring high acuity (i.e. grazers and slow-moving organisms) having lower SRP values (3–8 cycles per degree) [Collin and Pettigrew, 1989]. Very low SRP could also reflect a low reliance on vision in prey/predator interactions and indicate the use of other sensory systems [Bailes et al., 2006a]. In a relatively dark environment, where inter-specific interactions are mostly achieved through bright, bioluminescent flashes, as found in the mesopelagic zone, sensitivity may have become more important than acuity. As most lanternfishes possess very sensitive eyes [de Busserolles et al., 2014b], prey detection at longer distances is most likely achieved by the detection of a light signal or through the use of other sensory systems (olfaction or audition), with acuity only playing a role at close range.

Putative Function of the Amacrine Cell Population

Amacrine cells are usually present in the inner nuclear layer. However, amacrine cells have also been identified in the ganglion cell layer of several vertebrates (cats [Wong and Hughes, 1987], rabbits [Vaney et al., 1981] and newts [Ball and Dickson, 1983], including teleosts such as dragonets [van Haesendonck and Missotten, 1987], tench and rainbow trout [Weruaga et al., 2000], hake [Bozzano and Catalán, 2002] and cichlids [Mack et al., 2004]) and for this reason have been referred to as 'displaced' amacrine cells, although they appear to be a typical inclusion.

A large population of displaced amacrine cells was also identified in the ganglion cell layer of myctophids. Contrary to what has usually been found in other vertebrate retinas [Wong and Hughes, 1987; Collin and Pettigrew, 1988c; Bozzano and Catalán, 2002; Bailes et al., 2006b], the inclusion of the amacrine cell population in the total neural counts of cells within the ganglion cell layer in myctophids, which comprised up to 80% of the total neural cells in the ganglion cell layer, masked the distribution of ganglion cells. As ganglion cells are the only neurons possessing axons sending information to the visual centres of the brain, it is essential to exclude the amacrine cell population when assessing neuron distribution in order to unravel the true distribution and peak density of the ganglion cells (at least in myctophids).

Similar to the retina of cats [Wong and Hughes, 1987], rabbits [Vaney et al., 1981] and cichlids [Mack et al., 2004], the extremely large proportion of amacrine cells in

the ganglion cell layer of the lanternfish retina cannot be regarded as displaced and must represent a true cell population within the ganglion cell layer to serve a particular function. Mack et al. [2004] suggested that amacrine cells present in the ganglion cell layer probably have a strong influence on the output activity of the ganglion cells due to their proximity. Amacrine cells, in general, are in contact with every class of neuron with the exception of the photoreceptors, and many different types of amacrine cells exist (around 40 in teleosts) [Wagner and Wagner, 1988]. However, the functional role of many of these types is still unknown.

Anti-parvalbumin, the antibody used in this study to label amacrine cells, is well known for labelling a particular type of amacrine cell, i.e. AII amacrine cells, as described in several vertebrate retinas (in bats [Jeon et al., 2007], rabbits [Casini et al., 1995], rats [Wässle et al., 1993], cats [Gabriel and Straznicky, 1992], and cichlids [Mack et al., 2004]). AII amacrine cells are usually involved in the rod signal pathway and may improve the perception of small luminous objects against a dark background by quickening the usually slow rod response [Nelson, 1982]. Judging from the different labelling intensity, several types of amacrine cells might occur in the lanternfish retina. Wässle et al. [1993] also found 2 different populations of amacrine cells labelled with parvalbumin in the rat retina, i.e. AII amacrine cells and widefield amacrine cells. In lanternfishes, AII cells, if their presence is confirmed, might facilitate the detection of small bioluminescent flashes against the mesopelagic background, especially in the peripheral visual field, where they are most abundant.

Inter-Specific Differences in Retinal Specialisations in Lanternfishes: Ecology or Phylogeny?

The study of retinal topography in a large number of vertebrates, and more particularly mammals, has given rise to 2 main theories to explain the evolution of retinal specializations: the terrain theory by Hughes [1977] and the ancestry theory by Stone [1983]. While the terrain theory of Hughes [1977] suggests that retinal topography results from an adaptation of each species to the symmetry and openness of their perceived environment (habitat), the theory of Stone [1983] places more emphasis on the influence of evolutionary history, where a part of the retinal specialization is inherited from a common ancestor.

The strong phylogenetic signal highlighted in this study, which reveals that a similar type of retinal specialization is found in closely related species, supports the large influence of evolutionary history on retinal specializations. However, the presence of an elongated area ventro-temporalis, observed in several species, also indicates a clear adaptation to the mesopelagic environment by allowing the detection of silhouettes against the lighter background of the upper mesopelagic zone illuminated by downwelling sunlight and may indicate the influence of ecological and behavioural factors. Furthermore, most species possessing an elongated area are also known to be surface migrants and have been recorded in the first few metres of water at night (i.e. *Myctophum* sp., *Symbolophorus* sp., *D. laternatus* [de Busserolles et al., 2013]), where a weak visual horizon would be formed by the downwelling light emitted by the moon and stars or by the air-water interface, explaining the need for a streak-like elongated area in these species.

As recently demonstrated in a terrestrial vertebrate, i.e. the giraffe [Coimbra et al., 2013], and an amphibious vertebrate, i.e. the penguin [Coimbra et al., 2012], our findings support both theories and retinal specializations in myctophids appear to be driven by both ecology and phylogeny. However, more information on the ecology and behaviour of each species will be necessary to better understand the evolution of the visual system in lanternfishes and answer the following question: has the visual system of each lanternfish species adapted to a particular lifestyle or did each species develop different behaviours based on an inherited retinal arrangement? If the type of retinal specialization is really inherited from a common ancestor, then some predictions could be made on the possible visual capabilities of other myctophid species.

Acknowledgements

We wish to thank Dr. Mike Hall (AIMS) and the masters and crews of the RV Cape Ferguson, and Prof. Hans-Joachim Wagner (University of Tübingen) and the masters and crews of the FS Sonne for sea time opportunities. We thank Prof. Lynnath Beckley (Murdoch University), Dr. Brigitte Guillaumont (Ifremer) and Dr. Adrian Flynn (The University of Queensland) for providing additional samples. We gratefully acknowledge John Paxton (Australian Museum) for providing most of the fish identification, and Adrian Flynn, Caroline Kerr and Alan Goldizen for their help during field trips. We are indebted to Joao Paolo Coimbra for his assistance with retinal wholemount preparation, immunohistochemistry and stereology analyses and to Eduardo Garza-Gisholt for his help in using his R scripts for the creation of the topographic maps. This work was funded by the Australian Research Council (Discovery Grant to S.C., the Linkage Grant to N.J.M. and S.P.C.) and the West Australian State Government (S.P.C.). F.d.B. was supported by a Scholarship for International Research Fees and a University International Stipend at The University of Western Australia.

References

Baddeley A, Turner R (2005): Spatstat: an R package for analyzing spatial point patterns. J Stat Softw 12:1–42.

Bailes HJ, Robinson SR, Trezise AEO, Collin SP (2006a): Morphology, characterization, and distribution of retinal photoreceptors in the Australian lungfish *Neoceratodus forsteri* (Krefft, 1870). J Comp Neurol 494:381–397.

Bailes HJ, Trezise AEO, Collin SP (2006b): The number, morphology, and distribution of retinal ganglion cells and optic axons in the Australian lungfish *Neoceratodus forsteri* (Krefft 1870). Vis Neurosci 23:257–273.

Ball AK, Dickson DH (1983): Displaced amacrine and ganglion cells in the newt retina. Exp Eye Res 36:199–213.

Bozzano A, Catalán I (2002): Ontogenetic changes in the retinal topography of the European hake, *Merluccius merluccius:* implications for feeding and depth distribution. Mar Biol 141: 549–559.

Bozzano A, Collin SP (2000): Retinal ganglion cell topography in elasmobranchs. Brain Behav Evol 55:191–208.

Bozzano A, Pankhurst PM, Sabatés A (2007): Early development of eye and retina in lanternfish larvae. Vis Neurosci 24:423–436.

Case JF, Warner J, Barnes AT, Lowenstine M (1977): Bioluminescence of lantern fish (Myctophidae) in response to changes in light intensity. Nature 265:179–181.

Casini G, Rickman DW, Brecha NC (1995): AII amacrine cell population in the rabbit retina: identification by parvalbumin immunoreactivity. J Comp Neurol 356:132–142.

Coimbra JP, Hart NS, Collin SP, Manger PR (2013): Scene from above: retinal ganglion cell topography and spatial resolving power in the giraffe *(Giraffa camelopardalis)*. J Comp Neurol 521:2042–2057.

Coimbra JP, Marceliano MLV, Andrade-da-Costa BLS, Yamada ES (2006): The retina of tyrant flycatchers: topographic organization of neuronal density and size in the ganglion cell layer of the great kiskadee *Pitangus sulphuratus* and the rusty margined flycatcher *Myiozetetes cayanensis* (aves: Tyrannidae). Brain Behav Evol 68:15–25.

Coimbra JP, Nolan PM, Collin SP, Hart NS (2012): Retinal ganglion cell topography and spatial resolving power in penguins. Brain Behav Evol 80:254–268.

Coimbra JP, Trévia N, Marceliano MLV, Andrade-Da-Costa BLS, Picanço-Diniz CW, Yamada ES (2009): Number and distribution of neurons in the retinal ganglion cell layer in relation to foraging behaviors of tyrant flycatchers. J Comp Neurol 514:66–73.

Collin SP (1997): Specialisations of the teleost visual system: adaptive diversity from shallow-water to deep-sea. Acta Physiol Scand Suppl 638:5–24.

Collin S (1988): The retina of the shovel-nosed ray, *Rhinobatos batillum* (Rhinobatidae): morphology and quantitative analysis of the ganglion, amacrine and bipolar cell populations. J Exp Biol 47:195–207.

Collin SP (2008): A web-based archive for topographic maps of retinal cell distribution in vertebrates. Clin Exp Optom 91:85–95.

Collin SP, Hoskins RV (1997): Topographic mismatching of the displaced amacrine and ganglion cell populations in the retina of deep-sea lanternfish. Soc Neurosci Abstr 23:729.

Collin SP, Hoskins RV, Partridge JC (1997): Tubular eyes of deep-sea fishes: a comparative study of retinal topography. Brain Behav Evol 50:335–357.

Collin SP, Hoskins RV, Partridge JC (1998): Seven retinal specializations in the tubular eye of the deep-sea pearleye, *Scopelarchus michaelsarsi:* a case study in visual optimization. Brain Behav Evol 51:291–314.

Collin SP, Lloyd DJ, Wagner H-J (2000): Foveate vision in deep-sea teleosts: a comparison of primary visual and olfactory inputs. Philosophic Trans R Soc Lond B Biol Sci 355:1315–1320.

Collin SP, Partridge JC (1996): Retinal specializations in the eyes of deep-sea teleosts. J Fish Biol 49:157–174.

Collin SP, Pettigrew JD (1988a): Retinal topography in reef teleosts. 1. Some species with well-developed areae but poorly-developed streaks. Brain Behav Evol 31:269–282.

Collin SP, Pettigrew JD (1988b): Retinal topography in reef teleosts. 2. Some species with prominent horizontal streaks and high-density areae. Brain Behav Evol 31:283–295.

Collin SP, Pettigrew JD (1988c): Retinal ganglion cell topography in teleosts: a comparison between Nissl-stained material and retrograde labelling from the optic nerve. J Comp Neurol 276:412–422.

Collin SP, Pettigrew JD (1989): Quantitative comparison of the limits on visual spatial resolution set by the ganglion cell layer in twelve species of reef teleosts. Brain Behav Evol 34: 184–192.

Collin SP, Shand J (2003): Retinal sampling and the visual field in fishes; in Collin SP, Marshall NJ (eds): Sensory Processing in Aquatic Environments. New York, Springer, pp 139–169.

de Busserolles F, Fitzpatrick JL, Marshall NJ, Collin SP (2014b): The influence of photoreceptor size and distribution on optical sensitivity in the eyes of lanternfishes (Myctophida). PLoS One 9:e99957.

de Busserolles F, Fitzpatrick JL, Paxton JR, Marshall NJ, Collin SP (2013): Eye-size variability in deep-sea lanternfishes (Myctophidae): an ecological and phylogenetic study. PLoS One 8:e58519.

de Busserolles F, Marshall NJ, Collin SP (2014a): The eyes of lanternfishes (Myctophidae, teleostei): novel ocular specialisations for vision in dim light. J Comp Neurol 522:1618–1640.

Edwards AS, Herring PJ (1977): Observations on the comparative morphology and operation of the photogenic tissues of myctophid fishes. Mar Biol 41:59–70.

Fritsches KA, Marshall NJ, Warrant EJ (2003): Retinal specializations in the blue marlin: eyes designed for sensitivity to low light levels. Mar Freshw Res 54:333–341.

Gabriel R, Straznicky C (1992): Immunocytochemical localization of parvalbumin- and neurofilament triplet protein immunoreactivity in the cat retina: colocalization in a subpopulation of AII amacrine cells. Brain Res 595:133–136.

Garza-Gisholt E, Hemmi JM, Hart NS, Collin SP (2014): A comparison of spatial analysis methods for the construction of topographic maps of retinal cell density. PLoS One 9:e93485.

Glaser EM, Wilson PD (1998): The coefficient of error of optical fractionator population size estimates: a computer simulation comparing three estimators. J Microsc 192:163–171.

Haddock SHD, Moline MA, Case JF (2010): Bioluminescence in the sea. Annu Rev Mar Sci 2: 443–493.

Herring PJ (1985): How to survive in the dark: bioluminescence in the deep sea. Symp Soc Exp Biol 39:323–350.

Herring PJ (2002): The Biology of the Deep-Sea. New York, Oxford University Press.

Herring PJ (2007): Sex with the lights on? A review of bioluminescent sexual dimorphism in the sea. J Mar Biol Assoc UK 87:829–842.

Hughes A (1975): A quantitative analysis of the cat retinal ganglion cell topography. J Comp Neurol 163:107–128.

Hughes A (1977): The topography of vision in mammals of contrasting life style: comparative optics and retinal organisation; in Crescitelli F (ed): Handbook of Sensory Physiology. Berlin, Springer, vol II/5, pp 613–756.

Jeon YK, Kim TJ, Lee JY, Choi JS, Jeon CJ (2007): AII amacrine cells in the inner nuclear layer of bat retina: identification by parvalbumin immunoreactivity. Neuroreport 18:1095–1099.

Karnella C (1987): Family Myctophidae, lanternfishes; in Gibbs RH, Krueger WH (eds): Biology of Midwater Fishes of the Bermuda Ocean Acre. Washington, Smithsonian Institution Press, pp 51–168.

Kristoffersen JB, Salvanes AGV (1998): Effects of formaldehyde and ethanol preservation on body and otoliths of *Maurolicus muelleri* and *Benthosema glaciale.* Sarsia 83:95–102.

Locket NA (1977): Adaptations to the deep-sea environment; in Crescitelli F (ed): Handbook of Sensory physiology. Springer, Berlin, vol II/5, pp 67–192.

Mack AF, Sussmann C, Hirt B, Wagner HJ (2004): Displaced amacrine cells disappear from the ganglion cell layer in the central retina of adult fish during growth. Invest Ophthalmol Vis Sci 45:3749–3755.

Matthiessen L (1882): Über die Beziehungen, welche zwischen dem Brechungsindex des Kernzentrums der Krystalllinse und den Dimensionen des Auges bestehen. Pflügers Arch 27:510–523.
Matthiessen L (1886): Über den physikalisch-optischen Bau des Auges der Cetacean und der Fische. Pflügers Arch 38:521–528.
Moser HG, Ahlstrom EH (1970): Development of lanternfishes (family Myctophidae) in the California Current. 1. Species with narrow-eyed larvae. Nat Hist Mus Los Angel Cty Sci Bull 7:1–145.
Moser HG, Ahlstrom EH (1972): Development of lanternfish, *Scopelopsis multipunctatus* Brauer 1906, with a discussion of its phylogenetic position in the family Myctophidae and its role in a proposed mechanism for the evolution of photophore patterns in lanternfishes. Fish Bull 70:541–564.
Moser HG, Ahlstrom EH (1974): Role of larval stages in systematic investigations of marine teleosts: the Myctophidae, a case study. Fish Bull 72:391–413.
Nafpaktitis BG (1978): Systematics and distribution of lanternfishes of the genera *Lobianchia* and *Diaphus* (Myctophidae) in the Indian Ocean. Nat Hist Mus Los Angel Cty Sci Bull 30:1–92.
Nafpaktitis BG, Backus RH, Craddock JE, Haedrich RL, Robison BH, Karnella C (1977): Family Myctophidae; in Gibbs RH Jr, Berry FH, Böhlke JE, Cohen DM, Collette BB, Eschmeyer WN, Mead GW, Merriman D, Pietsch TW (eds): Fishes of the Western North Atlantic – Memoir of the Sears Foundation for Marine Research. New Haven, Yale University, vol 1, pp 13–265.
Nafpaktitis BG, Nafpaktitis M (1969): Lanternfishes (family Myctophidae) collected during cruises 3 and 6 of the R/V Anton Bruun in the Indian Ocean. Nat Hist Mus Los Angel Cty Sci Bull 5:1–79.
Nelson R (1982): AII amacrine cells quicken time course of rod signals in the cat retina. J Neurophysiol 47:928–947.
Paxton JR (1972): Osteology and relationships of the lanternfishes (family Myctophidae). Nat Hist Mus Los Angel Cty Sci Bull 13:1–81.
Paxton JR, Ahlstrom EH, Moser HG (1984): Myctophidae: relationships; in Moser HG, Richards WJ, Cohen DM, Fahay MP, Kendall AW, Richerdson SL (eds): Ontogeny and Systematic of Fishes. La Jolla, American Society of Ichthyologists and Herpetologists, vol 1, pp 239–244.
Podrazhanskaya SG (1993): Feeding habits of mesopelagic species of fish and estimation of plankton graze in the northwest Atlantic. Sci Counc Stud NAFO 19:79–85.
Slomianka L, West MJ (2005): Estimators of the precision of stereological estimates: an example based on the CA1 pyramidal cell layer of rats. Neurosci 136:757–767.
Stone J (1981): The Whole Mount Handbook: a Guide to the Preparation and Analysis of Retinal Whole Mounts. Sydney, Maitland.
Stone J (1983): Parallel processing in the visual system. New York, Plenum Press, p 438.
Ullmann JFP, Moore BA, Temple SE, Fernandez-Juricic E, Collin SP (2011): The retinal wholemount technique: a window to understanding the brain and behaviour. Brain Behav Evol 79: 26–44.
Vaney DI, Peichl L, Boycott BB (1981): Matching populations of amacrine cells in the inner nuclear and ganglion cell layers of the rabbit retina. J Comp Neurol 199:373–391.
van Haesendonck E, Missotten L (1987): Displaced small amacrine cells in the retina of the marine teleost *Callionymus lyra* L. Vision Res 27:1431–1443.
Wagner H-J (2001): Sensory brain areas in mesopelagic fishes. Brain Behav Evol 57:117–133.
Wagner H-J, Fröhlich E, Negishi K, Collin SP (1998): The eyes of deep-sea fish. 2. Functional morphology of the retina. Prog Retin Eye Res 17:637–685.
Wagner H, Wagner E (1988): Amacrine cells in the retina of a teleost fish, the roach *(Rutilus rutilus):* a Golgi study on differentiation and layering. Phil Trans R Soc Lond B Biol Sci 321: 263–324.
Walls GL (1942): The vertebrate eye and its adaptive radiation. Bloomfield Hills, The Cranbrook Institute of Science.
Wässle H, Grünert U, Röhrenbeck J (1993): Immunocytochemical staining of AII-amacrine cells in the rat retina with antibodies against parvalbumin. J Comp Neurol 332:407–420.
Watanabe H, Moku M, Kawaguchi K, Ishimaru K, Ohno A (1999): Diel vertical migration of myctophid fishes (family Myctophidae) in the transitional waters of the western North Pacific. Fish Oceanogr 8:115–127.
Weruaga E, Velasco A, Brinon JG, Arevalo R, Aijon J, Alonso JR (2000): Distribution of the calcium-binding proteins parvalbumin, calbindin D-28k and calretinin in the retina of two teleosts. J Chem Neuroanat 19:1–15.
West MJ, Slomianka L, Gundersen HJG (1991): Unbiased stereological estimation of the total number of neurons in the subdivisions of the rat hippocampus using the optical fractionator. Anat Rec 231:482–497.
Wong ROL, Hughes A (1987): The morphology, number, and distribution of a large population of confirmed displaced amacrine cells in the adult cat retina. J Comp Neurol 255:159–177.
Zahuranec BJ (2000): Zoogeography and systematics of the lanternfishes of the genus *Nannobrachium* (Myctophidae: Lampanyctini). Smithson Contrib Zool 607:1–69.